

SAR Sea Ice Discrimination Using Texture Statistics: A Multivariate Approach

David G. Barber and Ellsworth F. LeDrew

Earth Observations Laboratory, Institute for Space and Terrestrial Science, Department of Geography, University of Waterloo, Waterloo, Ontario N2L 3G1, Canada

ABSTRACT: Discrimination of sea ice classes using texture statistics derived from the conditional joint probability density functions of the grey level co-occurrence matrix (GLCM) is reported on. Univariate and multivariate analyses are used to describe the separability of synthetic aperture radar (SAR) sea ice feature space. Impact of the conditional parameters δ (interpixel sampling distance) and α (orientation), and the effect of adaptive filtering, are measured for distributions arising from five GLCM texture statistics. Results show that the effects of δ , α , and adaptive filtering are captured in each texture statistic's distribution. Multivariate classification accuracies are dependent on the number of texture statistics used in computation of the discriminant functions, and whether training or cross validation sets are used. Maximum discrimination is obtained when three texture statistics are used with α parallel to the look direction and δ at an interpixel sampling distance of one.

INTRODUCTION

THE 1990s COULD BE CONSIDERED the decade of synthetic aperture radar (SAR). Over the next five years three orbital SAR sensors will be launched: RADARSAT (Canada), ERS-1 (Europe), and JERS-1 (Japan). The imagery from these orbital platforms is expected to contribute significantly to a variety of resource management applications. Of particular relevance to this study are the plans to use data from these sensors for measurement and monitoring of sea ice. Within the international sea ice community these data will provide information on a range of issues from real time ice breaker tactical support to assessment and monitoring of climate change in the polar regions. Considering that RADARSAT is expected to have downlink rates between 80 and 105 megabits per second (N. Denyer, ERS-1 Project Manager, Canada Centre for Remote Sensing, pers. comm.), the requirement for semi-automated feature extraction (at the very minimum) is evident.

In this paper we investigate the potential of a particular texture algorithm for discrimination of SAR sea ice classes. Various approaches to scene understanding using tone and/or texture for SAR sea ice classifications are reviewed. A candidate texture algorithm is selected and evaluated, using rigorous statistical testing, for a variety of ice classes in a single scene. We believe that such testing is a necessary component of algorithm evaluation, and is particularly important for inter-algorithm comparisons.

SAR BACKSCATTERING FROM SEA ICE

Tone is created in a SAR image by point measurements of the backscattering coefficient (σ^0) and is largely a function of the size interrelationships between the radar wavelength and the scattering elements within a single pixel footprint. Texture refers to the spatial variation of tonal elements as a function of scale (Haralick *et al.*, 1973). Within a digital image a homogeneous texture field consists of a spatial arrangement of grey levels which are more homogeneous (as a unit) within than between texture fields.

The image data consists of a backscattering signal convolved with a coherent fading signal (Ulaby *et al.*, 1986). Fading is the constructive and destructive interference of coherent electromagnetic radiation. The results of fading are manifested in digital imagery as speckle, which is visually recognized as an increased frequency of light and dark pixels in what should be a relatively homogeneous grey level field. The statistics of

coherent fading are well understood (Ulaby *et al.*, 1986). If we account for the fading component of image variance, the remaining image texture is primarily a function of the near surface characteristics (e.g., in the case of sea ice: ice roughness, bubble density, temperature, snow cover, and brine volume). Image texture provides information which can be directly correlated with observable physical characteristics because different suites of these characteristics are associated with different ice types.

The texture component of σ^0 from sea ice is a combination of surface and volume scattering. Although seasonality has a large impact on the dielectric properties of sea ice and its snow cover and, therefore, σ^0 , a winter sea ice scene is largely dominated by surface scattering from young ice forms and volume scattering from the bubble matrix in the upper layer of multi-year ice forms (Kim *et al.*, 1985; Ulaby *et al.*, 1986). With the onset of melt, surface characteristics and the dielectric properties of the ice/snow change, resulting in significant changes in the radar return from a given ice type (Livingstone *et al.*, 1987).

System parameters such as frequency, polarization, and incidence angle also play an important role in the amount of backscattered radiation that is received by the SAR antenna, and on the spatial arrangements of the grey levels (i.e., texture) in the SAR scene. Modeling studies have provided valuable information on the optimal radar parameters for sea ice. Although a detailed account is beyond the scope of this paper, excellent reviews are available on the relative merits of system parameters (Kim *et al.*, 1985), seasonality (Livingstone *et al.*, 1987), and the contribution of different sea ice geophysical parameters (Ulaby *et al.*, 1986) to sea ice backscatter.

TONAL AND TEXTURAL SEPARATION OF SAR SEA ICE CLASSES

Both tonal and textural information are available for discrimination of SAR sea ice classes. Regardless of the features used, a SAR sea ice classification scheme should, at the very least, be machine assisted. In addition, the algorithm should be robust to classifications of a variety of ice features, from the simple (discrimination of multi-year ice), to the complex (seasonally adjusted discrimination of a full range of ice types from nilas to multi-year). In this section we review some of the pioneering work on tonal and textural classifications specific to SAR imagery of sea ice.

Before 1978, optical processing was the standard form for creating a SAR image from the signal data. This analog method was not sufficiently reproducible to allow classifications based solely on the backscattering coefficient (σ^0). With the advent of

digital processing techniques, and general improvements in radar imaging science, inter-image calibration has risen to a level where the calibration between images from the same sensor may be as close as 1dB (Raney, 1989). Given this high level of relative calibration, we can now consider the possibilities of a universal classification scheme.

SAR tonal statistical distributions were explored by Lyden *et al.* (1984). They investigated the assumption that the sampling distributions of tone for first-year and multi-year ice could provide a means of parametric discrimination of these ice types. Even within a single image the statistical separations of these ice types were poor. Shuchman *et al.* (1989) provide a detailed analysis of tone and the utility of modeling these distributions as a method of classification. Comparison between these distributions, and a "general co-occurrence matrix" texture measure, indicated that no improvement in discrimination is realized with the computationally more intensive texture measures. Unfortunately, no statistical precision measures were provided, and comparative analysis was restricted to visual interpretation of scatterplots. Further analysis by these authors is in progress, and they suggest that more quantitative evidence on the relative differences between tonal and textural measures will be forthcoming (Shuchman *et al.*, 1989).

Variations on simple image tone have also met with some success. Burns *et al.* (1982) used a median filter to reduce the contribution of fading to the overall image variance. By taking the deviation about the mean of a convolution window, it was possible to represent the texture contained within that window, independent of the contribution of coherent fading. Heolbaek-Hansen (1989) found that local variance of a filtered image provided a marginal improvement in classification accuracies over using just tone. Barber (1989) found that using deviations about the center pixel (Irons and Petersen, 1981) of a convolution window provided statistically separable signatures between first-year and multi-year ice forms. New ice could not be separated from first-year and land could not be separated from multi-year. In each of these studies, it was apparent that the separation of young ice from multi-year ice was not difficult. The problem occurs in separating similar scattering surfaces (*i.e.*, first-year rough versus first-year smooth or multi-year rough versus multi-year smooth).

In an attempt to separate the visually distinct textures within a SAR image, analysts began using digital algorithms which made use of more complex representations of texture. One such technique considers the computation of a co-occurrence matrix (also denoted as the grey level co-occurrence matrix or GLCM). This approach considers the spatial orientation of grey levels within a convolution window and has met with some success in a variety of remote sensing applications (Weszka *et al.*, 1976; Shanmugan *et al.*, 1981; Ulaby *et al.*, 1986; Pultz and Brown, 1987; Barber and LeDrew, 1989). Holmes *et al.* (1984) found that point statistics from the grey level co-occurrence matrix (GLCM) could provide discrimination of first-year, first-year ridged, multi-year, and multi-year rough sea ice. Classification accuracies, however, were on the order of 50 to 60 percent, lower than what could be considered operationally useful. Shokr (1989) conducted a preliminary investigation into the application of five texture statistics from the GLCMs. He found that these texture statistics were more robust to changes in tone between image dates and sensor frequencies when compared with simple tone.

In recent work by the authors (Barber *et al.*, 1990) analysis of the robustness of tonal versus GLCM textural classifications of sea ice were evaluated using data from two coincident images of Mould Bay, NWT. These analyses showed that tone was not as robust to variations in grey level created by differences in the look direction of the SAR when imaging the same ice surface. The robustness of tone versus texture was evaluated by

generating the classifier in one image (calibration data) and then directly applying it to the second image (validation data). Discriminant functions generated from multiple GLCM texture statistics provided consistently better agreement between the calibration and validation data sets than did tone.

The results of the tonal and textural classifications reviewed above are conclusive only within the limited range of conditions from which they were computed (*i.e.*, image date, specific frequency and polarization, etc). Given the importance (and immediacy) of a digital SAR sea ice classification algorithm, the literature provides a surprisingly limited amount of tangible information which can be used in selecting an appropriate classification scheme. We suspect the primary cause is that, historically, SAR imagery (particularly imagery with concurrent surface validation data) were limited in availability. There are, however, several commonalities apparent within these pioneering studies:

- It is generally regarded that a monotonically invariant classifier is required because of SAR calibration problems (Luther *et al.*, 1982; Lyden *et al.*, 1984; Holmes *et al.*, 1984) and because of backscatter reversals with seasonal change (Livingstone *et al.*, 1987). Improvements in the absolute and relative calibrations of aerial and future orbital SARs means that a tonal classification component will become increasingly important. Modeling efforts (Kim *et al.*, 1985; Drinkwater and Crocker, 1988), an attempt to implement a σ^0 look-up table for classifications at the Alaska SAR facility (Holt *et al.*, 1989) based on measured tonal distributions (Shuchman *et al.*, 1989), and the RIPLIB (Radar Image Processing LIBRARY) concept proposed by Shokr (1989) for the ERS-1 algorithm at the Ice Centre, Environment Canada, are valuable additions to the traditional, scene dependent, empirical digital image classification algorithm research.
- Previous research suggests that tonal classifiers are as accurate as textural classifiers but not as robust to differences in tone created by changes in look direction of the SAR imagery (Barber *et al.*, 1990). A rigorous statistical analysis of the precision of either approach has, however, not been adequately addressed, either within a single scene or between scenes.
- The utility of multivariate classifications using either, or both, tone and texture have not been adequately explored.
- Texture measures, either as local variance measures or as spatial grey level dependence methods, require further investigation (Holmes *et al.*, 1984; Lyden *et al.*, 1984; Burns and Lyzenga, 1984; Shokr, 1989; Hirose, 1989; Barber, 1989). The most promising features of these measures are their invariance to monotonic transforms of the grey level distributions within and between SAR images and the ability to measure a directionally dependent texture component.
- The research conducted to date is limited by a lack of imagery of the same scene from different seasons concurrent with surface validation data. Modelers are attempting to predict the type and range of backscattering we can expect from different ice types in different seasons, but empirical investigations, which are required to validate these findings, are limited in time (*i.e.*, results are extrapolated to general conditions for a given season and geographic location). This deficiency will soon be rectified with the launch of ERS-1 in 1991 and through continued analysis of *in situ* data coincident with aerial and orbital SAR imagery of sea ice from different regions and seasons.
- Results from the classification of a single image cannot be considered a universal truth. General trends are emerging, but universality of an algorithm for consistent separation of SAR sea ice feature space, or the extraction of geophysical properties of sea ice, is not imminent.

SELECTING A TEXTURE CLASSIFICATION APPROACH

In this analysis we focus on the utility of second-order texture measures for classification of ice types in SAR imagery. There are many approaches to second-order texture measures including statistical, structural, stochastic, and frequency domain analysis (Burns and Lyzenga, 1984; Sun and Wee, 1982; Connors and Harlow, 1980b; Weszka *et al.*, 1976; Haralick *et al.*, 1973).

Statistical approaches make use of grey level probability density functions (pdf). The pdf is usually computed as the conditional joint probability of pairs of pixel grey levels in a local area of the image. The grey level co-occurrence matrix (GLCM) (Haralick *et al.*, 1973), grey level run lengths (Galloway, 1975), and the neighboring grey level dependence matrix (Sun and Wee, 1982) are examples of statistical approaches to texture analysis.

Structural approaches exploit the notion of a texture primitive. These approaches generally consist in finding a texture primitive, extracting a set of features which characterize this primitive, then defining a placement rule for these primitives within the texture field of the image (Conners and Harlow, 1980b).

Stochastic approaches assume that texture fields can be estimated probabilistically based on a particular statistical model. The most commonly used models are based on Markov Chains (Hassner and Sklansky, 1980) or multidimensional random fields (Wechsler and Kidode, 1979).

Frequency domain analysis is based on the Fourier transform. Analysis is conducted in the frequency domain on the power spectra of the image. This approach is often called PSM (power spectrum method) (Conners and Harlow, 1980a). A variety of methods have been developed to separate different textures based on their power spectra (Roan and Aggarwal, 1987; D' Astous and Jernigan, 1984; and Matsuyama *et al.*, 1983).

With this multitude of approaches, and a general consensus among researchers that spatial information is important in feature classification, comparative studies have been conducted to determine which approach provides the best separation of feature space. Weszka *et al.* (1976) compared a frequency domain approach with first-order statistical measures and second order grey level co-occurrence probabilities. They found that the spatial domain approaches provided more precise classifications (both first-order difference measures and second-order grey level probabilities) than the frequency domain analysis. In a follow-up study, Conners and Harlow (1980a) conducted a rigorous theoretical analysis of the relative effectiveness of frequency domain analysis (power spectrum method, PSM), grey level co-occurrence matrices (GLCM) (Haralick *et al.*, 1973), grey level difference metrics (GLDM) (Weszka *et al.*, 1976), and grey level run lengths (GLRL) (Galloway, 1975). Conners and Harlow used synthetic texture fields based on Markov random fields. A major focus of the paper was to quantify the differences in each of the methods through all stages of the texture analysis, including a measure of the information content in the intermediary texture matrices versus the point statistics obtained from these matrices. They found that a significant loss of information occurs when a single point estimate is derived from the probability matrices (e.g., contrast, entropy, dissimilarity, etc.). Conners and Harlow (1980a) were able to ordinate the effectiveness of these four measures into GLCM, GLDM – and depending on the textures – GLRL, and PSM. Although these comparative analyses were not computed using sea ice texture fields, we feel the results of these analyses warrant a detailed evaluation of the GLCM, in particular, for separation of SAR sea ice classes.

GREY LEVEL CO-OCCURRENCE MATRICES (GLCMS)

Throughout this study we evaluate texture statistics derived from grey level co-occurrence matrices (GLCMs). A GLCM consists of a matrix which provides the conditional joint probabilities of all pairwise combinations of pixels within a computation window (W_{nm}). The co-occurrence of grey levels represent the probability of any two pairs of grey levels occurring, conditional on the interpixel sampling distance (δ) and orientation (α) used for computation. Algebraically this can be expressed as Equation 1 where C_{ij} is defined in Equation 2 following Haralick *et al.* (1973): i.e.,

$$Pr(x) = \{C_{ij}|\delta, \alpha\} \quad (1)$$

$$C_{ij} = \frac{P_{ij}}{\sum_{ij=1}^n P_{ij}} \quad (2)$$

where P is the frequency of occurrence of grey levels i and j . Summation over n refers to the total number of pixel pairs, which is dependent on the parameter δ and the subscripts n and m from W_{nm} .

In the following analyses an eight-bit image has been quantized to four to reduce computation time. Selection of the appropriate quantization level is essential to the precision of the texture classifier. Quantization will have a direct bearing on how much information is available for separation of the ice types. Kim *et al.* (1985) estimates a 20 dB difference between multi- and first-year ice under winter conditions at X band frequencies. Holmes *et al.* (1984) used a three-bit quantization for these conditions. In this study we have used a larger quantization, which requires more processing, in an effort to determine if more dynamic range will improve classification.

The texture statistics represent a single spatial measure of the image texture from which the GLCM is computed. Each texture statistic is considered a point estimate because it provides a single measure of the total information content of the GLCM. Five commonly used texture statistics (Barber and LeDrew, 1989; Pultz and Brown, 1987; Conners *et al.*, 1984; Shanmugan *et al.*, 1981) are used here:

Uniformity

$$\sum_{i=1}^n \sum_{j=1}^n C_{ij}^2 \quad (3)$$

Correlation

$$\sum_{i=1}^n \sum_{j=1}^n \frac{(i - \mu_x)(j - \mu_y) C_{ij}}{\sigma_x \sigma_y} \quad (4)$$

Entropy

$$\sum_{i=1}^n \sum_{j=1}^n C_{ij} \log C_{ij} \quad (5)$$

Dissimilarity

$$\sum_{i=1}^n \sum_{j=1}^n C_{ij} |i - j| \quad (6)$$

Contrast

$$\sum_{i=1}^n \sum_{j=1}^n C_{ij} (i - j)^2 \quad (7)$$

where

- σ_x = the standard deviation of row i ,
- σ_y = the standard deviation of column j ,
- μ_x = the mean of row i ,
- μ_y = the mean of column j , and
- n = the number of pixel pairs in the image at (α, δ) .

In this study we assess the characteristics of these texture statistics (point estimates) for discrimination of SAR sea ice features. Evaluation of each texture statistic, considered separately ('UNIVARIATE ANALYSIS'), provides comparative information on the discriminability of each texture statistic for separation of sea ice types. A multivariate evaluation, where several texture statistics are considered simultaneously ('MULTIVARIATE ANALYSIS'), is conducted through a linear discriminant analysis (LDA). This provides a means of evaluating the utility of the complimentary information contained within each additional texture statistic for discrimination of SAR sea ice types. Tests are

conducted to determine the impact of the GLCM conditional parameters δ (interpixel sampling interval), α (orientation), and adaptive filtering on textural discrimination in SAR images of sea ice.

UNIVARIATE ANALYSIS

The objective of this section is to describe the distributions of each texture statistic (Equations 3 to 7) within each of four ice types (new ice, first-year ice, multi-year ice, and land; Figure 1) and to determine if these distributions provide significant discrimination of ice types. We also evaluate changes in the distribution of the texture statistics due to the interpixel sampling interval (δ), orientation (α), and adaptive filtering of SAR imagery. Specifically, two research questions are addressed:

- (1) What is the effect of the interpixel sampling variable δ and orientation variable α on the distribution of each texture statistic?
- (2) What is the effect of adaptive filtering on the distribution of the texture statistics?

METHODS

A Sea Ice and Terrain Assessment Radar-1 (STAR-1) (Nichols et al., 1986) SAR image (Figure 1; Mould Bay, NWT, 3 March 1984) from the Canadian Radar Age/Type Algorithm Group (CRAGTAG) standardized image dataset, was used to create four images (Figure 2): two original 6m (seven look) and two, 6m adaptively filtered (6mf). This scene was acquired at incidence angles between 68.5 degrees and 78.9 degrees at X-band frequency and HH polarization. The sub-images are computed for an approximately two-degree incidence-angle range. Figures 1 and 2 are oriented with north to the top of the image; east and west are reversed (this is the standard format of digital STAR-1 imagery).

Filtering was considered necessary because of the contribution of coherent fading to image texture in the STAR-1 SAR scene. The 6mf images were produced using an adaptive filter (Equation 8) described in Durand *et al.* (1987) where the subscript nk denotes a 3 by 3 window and "hom" a homogeneous texture class.

$$\hat{X}_{ij} = \bar{X}_{nk} + (X_{ij} - \bar{X}_{nk}) \cdot (s_{nk}^2 - s_{\text{hom}}^2) / s_{nk}^2 \quad (8)$$

All ice classes were selected using a 25 by 25 window located randomly in the filtered and unfiltered sub-images (Figure 2). Surface validation was supplied by the Atmospheric Environment Service Ice Branch. During sample selection a subarea was accepted if it represented a homogeneous sample of an ice type of interest. This process was repeated without replacement until 15 homogeneous replicates of four ice types (new ice {NWI}, first-year ice {FYI}, multi-year ice {MYI}, and land {LAND}) were obtained. The GLCMs used in this analysis were computed on four-bit images at interpixel sampling distances ($\delta = 1, 5, 9$) and orientations ($\alpha = 0^\circ, 45^\circ, 90^\circ$). The $\alpha = 0^\circ$ is parallel to the range dimension of the scene (Figure 2). The mean and standard deviations for each of the texture statistic distributions were graphed to show separation of ice classes within each of the texture statistics (Figure 3).

Assessment of the first research question was conducted using analysis of variance (ANOVA). Differences attributable to δ and α were assessed using Scheffe's *post hoc* test for differences of factor means. This test determines the relative contribution of all pairwise combinations of factors to a significant F statistic. All variable sets were tested for the distributional assumptions of the parametric ANOVA. In all cases but one the assumptions were met. For the texture statistic 'Contrast' and class 'LAND', the variables were not sufficiently homoscedastic and were

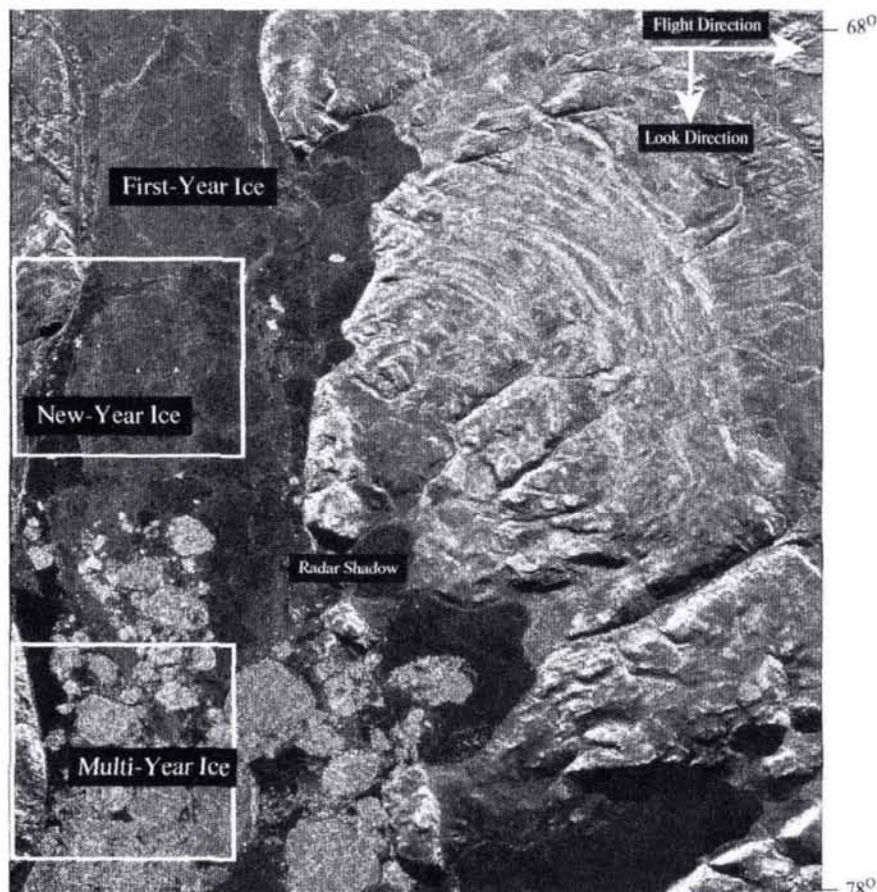


FIG. 1. Synthetic Aperture Radar image of Mould Bay, NWT (3 March 1984). Study sites are denoted by the white boxes (Figure 2). The four ice classes used in this study are overlain. Flight direction, look direction, and incidence angles are presented.

transformed by their square root before conducting the ANOVA. Interpretation of these *post hoc* results is specific to whether differences arise due to δ or α . If there is no difference in δ , then a saving in computation time can be realized by computing the GLCMs at a larger interpixel sampling distance. This assumes that $\delta = 1$ provides maximum information. The pairwise combinations are between the interpixel sampling distances 1, 5, and 9. Because SAR backscattering is predominantly a function of surface roughness for young ice types, and the combination of volume and surface scattering in multi-year ice types, directionality of a texture statistic may provide meaningful information on discrimination of texture classes based on the scattering structure relative to the radar range dimension. With young ice types this may be caused by the orientations and relative frequencies of small scale deformation. With multi-year ice forms, backscatter directional dependence may be created by the orientation of hummocks and the corresponding drainage networks of the melt ponds.

The second research question was designed to determine whether there is a significant difference between texture measurements of adaptively filtered and unfiltered replicates of the four ice types. Adaptive filtering reduces the local variation of a texture class as a function of the local mean. If the distributions are significantly different, then filtering can be considered to provide different information which may (or may not) be useful in classification. A series of two-tailed t-tests were conducted to measure the difference between the original and filtered texture statistic distributions of 15 replicates from the four ice classes.

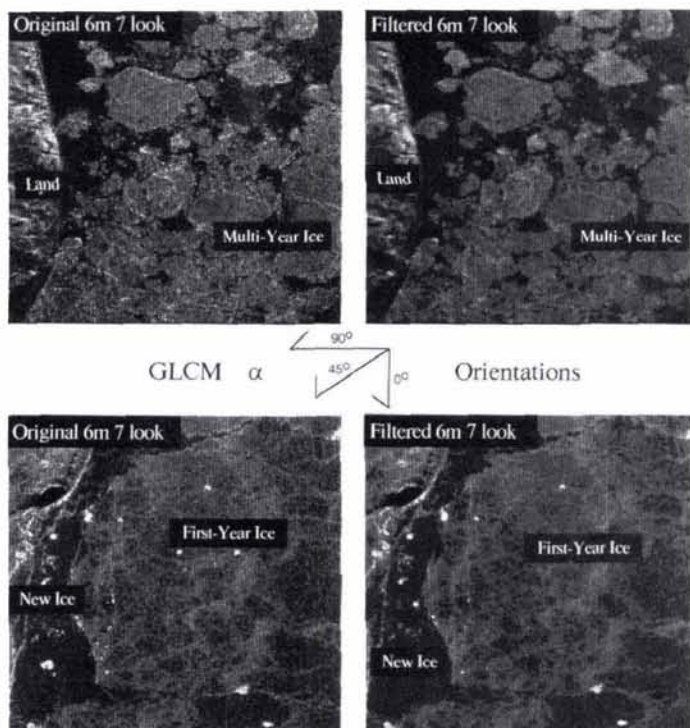


FIG. 2. Two study sites, extracted from Figure 1 (white boxes). Left side of the plate denotes the original imagery (6m; 7-look) and the right side shows the filtered imagery (also 6m; 7-look). These sub-images are oriented to the flight direction of the aircraft. Orientations of the GLCM parameter (α) are denoted between the sets of images. An $\alpha = 0^\circ$ is parallel to the look direction of the SAR. The ice types extracted from each scene are denoted.

RESULTS

The potential for using a single texture statistic for SAR sea ice classification is a function of the mean and standard deviation of that statistic's distribution (Figure 3). Separability is a function of the mean (X axis; Figure 3), precision of this separation is a function of the standard deviation (Y axis; Figure 3). As the relative standard deviation increases, the precision of any particular separation will decrease. It is apparent that each of the texture statistics provides different relative amounts of class separation.

Research Question One

What is the effect of the interpixel sampling variable δ and orientation variable α on the distribution of each texture statistic?

The symbol §, in the pairwise comparison columns (Tables 1 and 2) denote a significant difference between the title pair. The P value provides a measure of the significance of the analysis of variance. Specifically, the P value is the probability of concluding that there is a significant difference between the δ or α pairs when in reality there is not (Type I error). In terms of hypothesis testing, we reject the null hypothesis that the α and δ pairs are equal for all Type I errors which are greater than the P value. The ANOVA tests the distributional differences between the three variables which arise from different α and δ for each texture statistic. There are four general results available from interpretation of Tables 1 and 2:

- Correlation and entropy are the least sensitive of the five texture statistics to δ (higher P values; Table 1)
- Land and multi-year ice are more sensitive to changes in δ than first-year ice and new ice (lower P values; Table 1).
- All the texture statistic are more sensitive to changes in α than to changes in δ (higher P values in Table 1 than Table 2).
- There is evidence to suggest that 0° and 45° orientations are more similar than the other pairwise combinations of α for the ice classes tested (lower frequency of significant differences for these pairs compared with the other pairs; Table 2).

Research Question Two

What is the effect of adaptive filtering on the distribution of the texture statistics?

Results of the t-tests indicate that information due to filtering

TABLE 1. DIFFERENCES DUE TO THE INTERPIXEL SAMPLING INTERVAL ($\delta = 1, 5, \text{ AND } 9$)

Statistic	Ice Type	P value	1vs5	1vs9	5vs9
Uniformity	First-Year Ice	0.260			
	New Ice	0.060			
	Land	0.003	§	§	
	Multi-Year Ice	0.001	§	§	
Correlation	First-Year Ice	0.060			
	New Ice	0.530			
	Land	0.450			
	Multi-Year Ice	0.160			
Entropy	First-Year Ice	0.240			
	New Ice	0.220			
	Land	0.047			
	Multi-Year Ice	0.001	§	§	
Dissimilarity	First-Year Ice	0.000	§	§	
	New Ice	0.001	§	§	
	Land	0.000	§	§	§
	Multi-Year Ice	0.000	§	§	§
Contrast	First-Year Ice	0.000	§	§	
	New Ice	0.001	§	§	
	Land*	0.000	§	§	§
	Multi-Year Ice	0.000	§	§	§

*This ANOVA was conducted on square root transformed variables to stabilize variances between the three levels of δ (see methods).

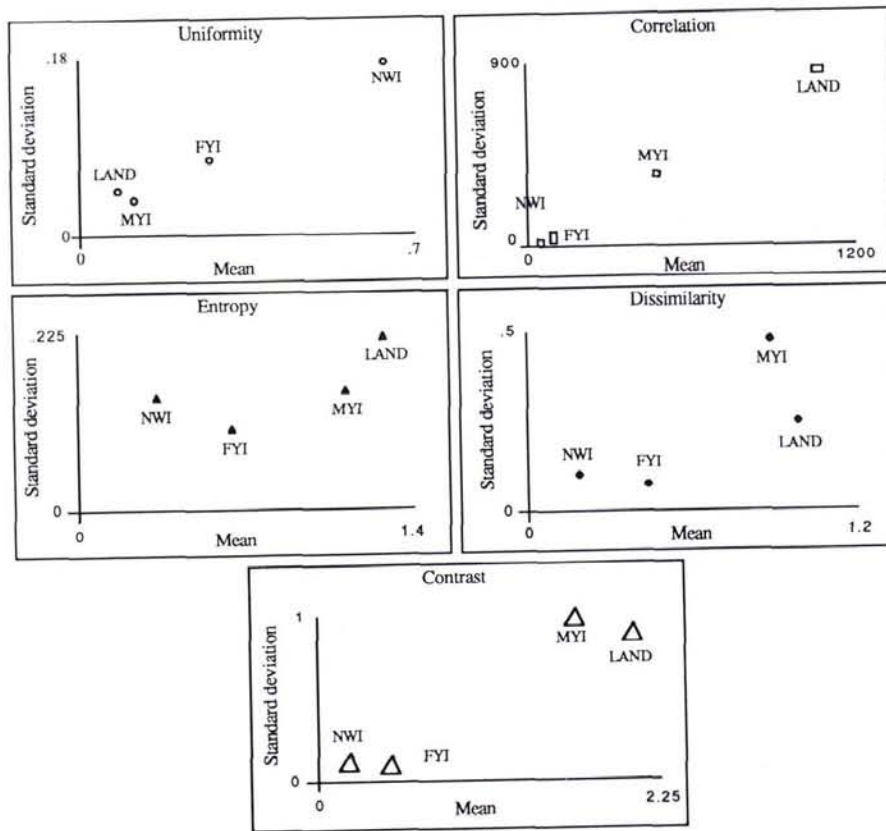


FIG. 3. Mean and standard deviation of 15 replicates from five texture statistics of four ice classes.

TABLE 2. DIFFERENCES DUE TO THE ORIENTATION PARAMETER ($\alpha = 0^\circ, 45^\circ, \text{ AND } 90^\circ$).

Statistic	Ice Type	P value	0° vs 45°	0° vs 90°	45° vs 90°
Uniformity	First-Year Ice	0.000		$\$$	$\$$
	New Ice	0.000	$\$$	$\$$	$\$$
	Land	0.000		$\$$	$\$$
	Multi-Year Ice	0.000		$\$$	$\$$
Correlation	First-Year Ice	0.000	$\$$	$\$$	$\$$
	New Ice	0.327		$\$$	$\$$
	Land	0.000		$\$$	$\$$
	Multi-Year Ice	0.000		$\$$	$\$$
Entropy	First-Year Ice	0.000		$\$$	$\$$
	New Ice	0.002	$\$$	$\$$	$\$$
	Land	0.000		$\$$	$\$$
	Multi-Year Ice	0.000		$\$$	$\$$
Dissimilarity	First-Year Ice	0.000	$\$$	$\$$	$\$$
	New Ice	0.000	$\$$	$\$$	$\$$
	Land	0.000	$\$$	$\$$	$\$$
	Multi-Year Ice	0.000		$\$$	$\$$
Contrast	First-Year Ice	0.000	$\$$	$\$$	$\$$
	New Ice	0.000	$\$$	$\$$	$\$$
	Land*	0.000		$\$$	$\$$
	Multi-Year Ice	0.000		$\$$	$\$$

TABLE 3. T-TEST RESULTS FROM THE DIFFERENCE BETWEEN ORIGINAL (ORIG) AND FILTERED (FILT) ICE CLASSES USING EACH OF THE FIVE TEXTURE STATISTICS

Ice Type	Texture Statistic	Mean (Orig-Filt)	t value	P. value
First-Year Ice	Uniformity	-0.105	-5.95	0.0001
	Correlation	9.540	5.06	0.0002
	Entropy	0.109	8.47	0.0001
	Dissimilarity	0.167	18.24	0.0001
	Contrast	0.191	12.38	0.0001
New Ice	Uniformity	-0.183	-10.85	0.0001
	Correlation	6.807	5.64	0.0001
	Entropy	0.153	13.06	0.0001
	Dissimilarity	0.116	9.12	0.0001
	Contrast	0.120	9.49	0.0001
Land	Uniformity	-0.032	-4.45	0.0005
	Correlation	140.130	3.77	0.0021
	Entropy	0.117	14.75	0.0001
	Dissimilarity	0.221	18.45	0.0001
	Contrast	0.619	11.27	0.0001
Multi-Year Ice	Uniformity	-0.053	-7.26	0.0001
	Correlation	63.130	11.75	0.0001
	Entropy	0.140	15.29	0.0001
	Dissimilarity	0.204	26.59	0.0001
	Contrast	0.473	12.92	0.0001

is captured by each of the texture statistics. The P value indicates the significance level of the differences between the original and filtered distributions for each texture statistic within a particular ice class (Table 3). Mean refers to the average difference between the original minus the filtered distributions (recall that there are 15 samples, each with 625 pixels, in each distribution). The t value is the statistic which is computed when comparing the two distributions. With the exception of new ice, the dissimilarity texture statistic was the most sensitive to the effect of adaptive

filtering (largest t value). The low P values for all ice types and texture statistics tested, indicate that the effect of adaptive filtering is highly significant (Table 3).

DISCUSSION

Significant differences occurred between distributions of GLCM texture statistics, computed at different levels of δ and α . The

changes due to δ are probably a result of the smaller sample sizes obtained at $\delta=5$ and 9. For a uniform texture (i.e., new ice), smaller sample sizes would not be as critical as for a more heterogeneous texture (i.e., land). Alignment of surface roughness elements relative to the incident angle of the radar may create structure within the rougher ice classes which is captured differently depending on the orientation used to compute the GLCMs.

Filtering resulted in a highly significant difference between distributions of GLCM texture statistics over all classes tested. Note that the mean difference of original minus filtered resulted in a negative value for each of the ice classes for the uniformity measure (Table 3). Recall from Equation 3 that uniformity is the squared summation of the conditional joint probability densities within each cell of the GLCM. By reducing the variation within each of the ice classes, the filtered GLCM will have fewer cells with positive probabilities, resulting in a higher uniformity measure. Entropy, dissimilarity, contrast, and to a lesser extent correlation all increase as the standard deviation of the image feature increases. The result is that the mean difference (Orig-Filt) is positive, confirming that the filter does reduce local variation.

These results show that changes caused by adaptive filtering are consistently captured by each of the GLCM texture statistics. We make no claims as to the utility of the significant differences due to δ and α , or those due to adaptive filtering, on discrimination of ice types. This analysis has shown that significant differences do occur; determining what the utility of these differences are on discrimination is the topic of the following section.

MULTIVARIATE ANALYSIS

It has been shown that the information contained within the GLCMs is not adequately captured by any single texture statistic (Connors and Harlow, 1980a). It is also apparent from the previous analysis (Figure 3) that each of the texture statistics provides different relative separation of the four ice classes. Close examination of Equations 3 to 7 shows that some of the variables will be highly correlated and others will not. The higher the correlation between pairwise variables, the less likely that selection of these variable pairs will improve discrimination (Table 4).

The primary objective of this section is to determine whether several texture statistics, considered in a multi-textural space, will provide good discrimination of sea ice classes. We will also assess the impact of the GLCM conditional parameters δ and α and the effect of adaptive filtering on the multivariate discrimination of SAR sea ice types. To meet these objectives, linear discriminant analysis (LDA) is used. Although maximum-likelihood estimation is a standard algorithm for classification, linear discriminant analysis (LDA) has also been used (Franklin *et*

al., 1989; Kershaw, 1987; Mather, 1987; Steiner *et al.*, 1971). LDA is commonly used to assess the contribution of several variables to classification precision (Blom *et al.*, 1987; Schwaller, 1987; Steiner *et al.*, 1971) or assessment of a set of variables to classification accuracy (Barber and LeDrew, 1989; Franklin *et al.*, 1989; Kershaw, 1987). Throughout this paper, precision will refer to the variability of repeated estimates and accuracy to the proximity of these estimates to the true population parameter.

We used LDA as a means for determining which set of p variables maximize discrimination of k ice classes. The number of discriminant functions which result is the smaller of $k - 1$ or p . LDA provides a set of linear transformations which maximize the inter- to intra-class variation over k . This is equivalent to maximizing the F ratio of a one way analysis of variance (Manly, 1986). The first function (Z_1) maximizes the inter- versus intra-class variation, over the entire data matrix. The second function (Z_2) maximizes the F ratio, with the important limitation that Z_2 is statistically orthogonal to Z_1 , and so on (Manly, 1986).

Computation of the discriminant functions can be conducted with all or a portion of the available training set. In this analysis, training set refers to those samples used to compute the discriminant functions. Cross validation refers to the difference between predicted (through the discriminant functions) and observed class assignments, from samples not used in the training set. The Mahalanobis distance (Manly, 1986) is the metric used to assign class probabilities. To specifically address the objectives of this section, four research questions are posed:

- (1) Do the conditional parameters δ and α affect discrimination?
- (2) Is there a difference between training and cross validation results?
- (3) What is the best set of texture statistics to discriminate SAR ice types?
- (4) What is the effect of adaptive filtering on discrimination accuracy?

METHODS

The methods of sample collection are consistent with those described in the 'UNIVARIATE ANALYSIS' section. Discriminant analysis was computed using a Macintosh II microcomputer, based on algorithms described in Ludwig *et al.* (1988) and using SYSTAT (Wilkinson, 1987). Computation of the discriminant functions (training set) was based on 15 samples unless stated otherwise in the results (i.e., training and cross validation in research question two).

Data used for analysis of each of the research questions are summarized (Table 5) into seven data sets (Set #); (Vars) is the number of texture statistics used in each trial; (α) and (δ) are the orientation and interpixel sampling distances used to generate the GLCMs; (Trials) is the number of sets of variables (i.e., Set #1 = 3 trials of 5 Vars.); (Selection) is either fixed (all possible) or random. To illustrate, consider set 1. There are five variables in this set (uniformity, correlation, entropy, dissimilarity, and contrast), each obtained at an orientation of 0° . Three trials are conducted with this set of variables, at the interpixel sampling distance of 1, 5, and 9. The trial at $\delta=9$ consists of all five texture

TABLE 4. CORRELATION STRUCTURE FROM UNIFORMITY, CORRELATION, ENTROPY, DISSIMILARITY, AND CONTRAST.

	Uniformity	Correlation	Entropy	Dissimilarity	Contrast
Uniformity	1				
Correlation	-.537	1			
Entropy	-.912	.776	1		
Dissimilarity	-.87	.809	.983	1	
Contrast	-.705	.856	.901	.951	1

TABLE 5. PARAMETERS CONTAINED IN EACH LDA DATASET.

Set #	Vars	Orientation (α)	Interpixel distance (δ)	Trials	Selection
1	5	0°	1,5,9	3	fixed
2	5	$0^\circ, 45^\circ, 90^\circ$	1	3	fixed
3	3	0°	1	5	random
4	5	0°	5	5	random
5	3	0°	9	5	random
6	10	0°	1,5,9	3	5 by 5
7	10	$0^\circ, 45^\circ, 90^\circ$	1	3	5 by 5

statistics at $\alpha=0^\circ$ and $\delta=9$. Set # is referenced in the response to each research question.

Contingency tables were tabulated for each set of variables. A k-hat statistic (Kappa Coefficient) and variance (Ks) of this statistic (Bishop *et al.*, 1975) were computed for each set of texture variables. Confidence intervals (C.I.) were computed based on an assumed normal distribution of the K-hat statistic at a 99 percent level against a Type I error (Upper and Lower C.I.). Hypothesis testing for research questions one and two was conducted using the confidence regions around the K-hat statistic. Selection of the most appropriate set of variables (question 3) was also based on these confidence regions. Wilkes Lambda ($W\lambda$) and the F statistic associated with each LDA is presented as additional information on the significance of each analytical result. The computational algorithms used, and a description of hypothesis conditions are reviewed by Manly (1986).

The impact of filtering was also tested using the K-hat confidence regions. To assist with interpretation of the results, the probabilities associated with each of the 60 samples used in one trial (15 samples of four ice types) are presented. The probabilities are derived from the Mahalanobis distance metric associated with each observation in the LDA. A moving average was used to smooth the probabilities so that trends, between filtered and unfiltered probabilities, could be interpreted from the line diagrams (Figures 4 and 5).

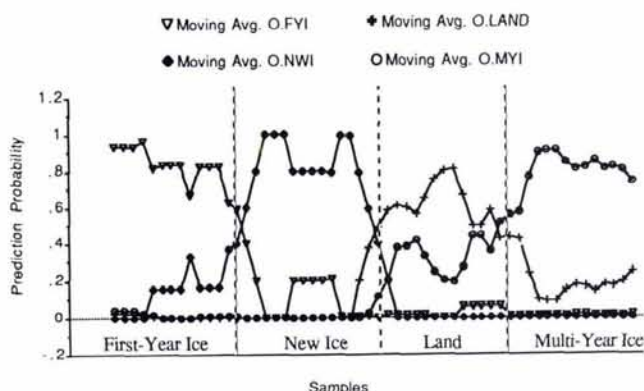


FIG. 4. Prediction probabilities derived from LDA of an unfiltered SAR image.

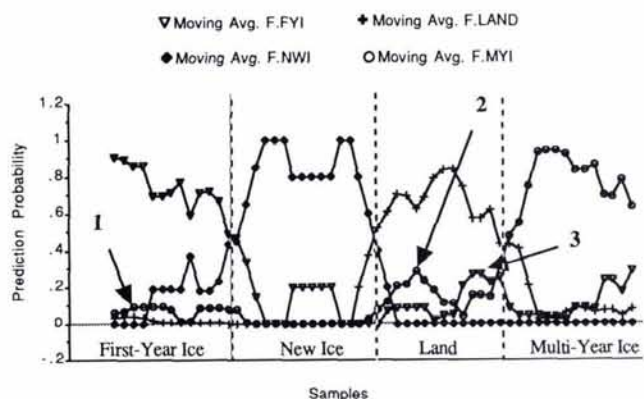


FIG. 5. Prediction probabilities derived from LDA of a filtered SAR image.

RESULTS

Research Question One

Do the conditional parameters δ and α affect discrimination?

Set 1 and 2 provide information pertinent to this research question. Set 1 consists of three sets of all five texture statistics (Equations 3 to 7) at $\{\delta, \alpha\} = \{1, 0^\circ\}; \{5, 0^\circ\}; \{9, 0^\circ\}$. Set 2 consists of all five texture statistics at $\{\delta, \alpha\} = \{1, 0^\circ\}; \{1, 45^\circ\}; \{1, 90^\circ\}$. A significant difference occurred between samples obtained at $\delta=1$ compared with observations at $\delta=5$ and 9 (Table 6). Also note that $\delta=5$ and 9 are not significantly different. Samples obtained at 0° are also significantly different than either $\alpha=45^\circ$ or 90° (Table 7). In set 2 the variables at $\alpha=45^\circ$ and 90° produced a significantly better result than set 1 variables at interpixel sampling distances of 5 and 9. This confirms the importance of obtaining information from every pixel regardless of the orientation used in the algorithm.

Research Question Two

Is there a difference between training and cross validation results?

Set 1 is used to assess the difference between training and cross validation discrimination accuracies. The two types of discrimination assessments were significantly different over all sets of variables tested (Table 8). The column 'Difference' (Table 8) is the minimum significant difference between the training and cross validation sets of each variable (i.e., Lower C.I. of training - Upper C.I. of cross validation). Training results are computed with five samples and cross validation with ten. The training set results are from 14.7 to 21.2 percent higher than those obtained through cross validation.

Research Question Three

What is the best set of texture statistics to discriminate SAR ice types?

Determining the most appropriate set is conducted by computing an LDA on all the variable sets (Set #; Table 9). Wilkes Lambda ($W\lambda$) and an F ratio derived from $W\lambda$ show the significance of each particular set, for discrimination of the four ice classes. Both training and cross validation discrimination

TABLE 6. DIFFERENCE IN CLASSIFICATION DUE TO δ .

Set #	Var set	K-Hat	Ks	Lower C.I.	Upper C.I.
1	$\delta=1$	82.2%	0.374%	81.1%	83.3%
1	$\delta=5$	75.6%	0.374%	74.4%	76.7%
1	$\delta=9$	77.8%	0.374%	76.7%	78.9%

TABLE 7. DIFFERENCE IN CLASSIFICATION DUE TO α .

Set #	Var set	K-Hat	Ks	Lower C.I.	Upper C.I.
2	$\alpha=0^\circ$	82.2%	0.374%	81.1%	83.3%
2	$\alpha=45^\circ$	77.8%	0.374%	76.7%	78.9%
2	$\alpha=90^\circ$	80.0%	0.374%	78.9%	81.1%

TABLE 8. CROSS VALIDATION AND TRAINING CLASSIFICATION ACCURACY FOR SET 1.

Sampling	Set#	Var set	K	Ks	Difference	Lower C.I.	Upper C.I.
Cross valid.	1	$\delta=1$	66.7%	0.927%		63.9%	69.4%
	1	$\delta=5$	60.0%	0.951%		57.1%	62.9%
	1	$\delta=9$	63.3%	0.878%		60.7%	66.0%
Training.	1	$\delta=1$	86.7%	0.857%	14.7%	84.1%	89.2%
	1	$\delta=5$	86.7%	0.857%	21.2%	84.1%	89.2%
	1	$\delta=9$	86.7%	0.834%	18.2%	84.2%	89.2%

TABLE 9. RESULTS OF ALL VARIABLE SETS FOR DISCRIMINATION OF ICE CLASSES.

Set#	Trials	Variables	WA	F	Training		Cross Validation	
					K-Hat	Ks	K-Hat	Ks
one	3	5	0.00	14.23	87.0%	0.85%	63.3%	0.92%
two	3	5	0.00	16.64	89.0%	0.69%	72.2%	0.79%
three	5	3	0.02	18.84	<u>90.6%</u>	0.55%	<u>69.3%</u>	0.83%
four	5	3	0.03	13.39	91.8%	0.51%	63.3%	0.89%
five	5	3	0.04	11.01	87.0%	0.80%	60.6%	0.93%
six	3	10	0.00	9.47	97.7%	0.14%	53.3%	1.20%
seven	3	10	0.00	10.02	97.7%	0.14%	62.2%	1.10%

accuracies are presented. These analyses show that substantial variability occurs in discrimination accuracies attributable to each set. Because there is no significant difference between set 2 ($\{\delta, \alpha\} = \{1, 0^\circ\}; \{1, 45^\circ\}; \{1, 90^\circ\}$) and set 3 (five trials each with three texture statistics at $\delta=1$ and $\alpha=0^\circ$), both provide the best discrimination of all sets tested (underlined values in Table 9). It is also interesting to note that agreement between training sample results and cross validation was higher when fewer variables were used (i.e., sets 3, 4, and 5).

Research Question Four

What is the effect of adaptive filtering on discrimination of ice types?

Analysis of the difference in the statistical distributions showed that adaptive filtering resulted in a significant difference for each texture statistic (Table 3). The impact of this change on classification accuracy is, however, not significant. At a 99 percent level against a Type I error, there is no significant difference between the average of five trials with three variables all at $\delta=1$ and $\alpha=0$ (Table 10). It would appear that the change in distribution of each measure recombinates in an unpredictable way, resulting in a non-significant difference between filtered and unfiltered images.

To provide illumination on this result, the probabilities from one of the sets within the original and filtered images were plotted (Figures 4 and 5). For each sample, a probability was computed from the Mahalanobis distance metric. Because each line is the average of five adjacent probabilities, the trends for each ice class (separated by dotted lines) and comparison of these trends between filtered (Figure 5) and unfiltered (Figure 4) can be readily observed. It is apparent that for each class the probabilities are highest for the correct samples. Confusion is high between multi-year ice and land both within the land class and within the multi-year class for the unfiltered images (Figure 4). Differences in the filtered versus unfiltered probabilities have been flagged with arrows to assist interpretation (Figure 5). Point 1 shows an increase in the probability of misclassification of MYI to FYI. This is accompanied by a corresponding decrease in the misclassification probabilities of MYI in the land class (point 2; Figure 5). Point 3 shows that FYI has a higher probability of being confused with both land and MYI when the imagery is filtered.

DISCUSSION

If we assume maximum information is obtained at $\delta=1$, then sampling at $\delta=5$ or 9 provides significantly less information than the former. Analysis of set 2 shows that $\delta=1$ provides significantly better results, regardless of orientation, than do larger interpixel sampling distances. It is interesting to note that 45° and 90° orientations provided significantly poorer results than 0° . Computation of the GLCM α parameters is graphically illustrated in Figure 2. The results of these analyses indicate (limited to the ice types and sensor conditions in the study) that significantly better classification accuracies were obtained when

TABLE 10. AVERAGE DISCRIMINATION ACCURACIES FOR SET 3, ORIGINAL AND FILTERED.

Sample	Var set	K	Ks	Lower C.I.	Upper C.I.	Significance
Original	Three	75.6%	0.4%	74.4%	76.7%	No
Filtered	Three	73.3%	0.4%	72.2%	74.5%	

the GLCM α parameter was parallel to the look direction of the sensor.

Cross validation results were substantially lower than training results. A likely cause for this is that the training sample accounts for an unrealistically high discrimination accuracy (K-hat = 86.7%, Ks = 0.857% for a training sample of five; and K-hat = 82.2%, Ks = 0.374% for a training sample of 15). The lower variance of the larger training set indicates that the sample size of five is too small to adequately represent the information contained within the ice texture samples.

To make a universal statement regarding the best set of texture statistics for discrimination of these ice types would be premature based on the natural variability observed within each discrimination result. Some general statements are perhaps more appropriate given the constraints of these analyses.

- Results are highly variable, depending on which texture set is used and whether we evaluate with the training or cross validation results.
- The best results (high K-hat for both training and cross validation) were obtained from sets with three texture variables.
- Sets 6 and 7 provide excellent training results but poor cross validation results. This is probably a function of the relationship between the number of variables used to compute the discriminant functions and the training sample size (for more information see Williams and Titus(1983)).

Filtering appears to confuse the boundaries between each of the ice classes in the context of the LDA. Figures 4 and 5 show a general increase in the probabilities of misclassification, particularly with FYI and MYI in the land class. Reasons for this difference are open to speculation. It may be that the adaptive filter reduces the variation of the rougher ice classes (MYI and land) so that these classes are more often confused with the more uniform textures of FYI and NWI. There is a definite increase in the probabilities of misclassification (Figure 5) even if there is no significant difference between filtered and unfiltered ice classifications (Table 10).

CONCLUSIONS

The conditional parameters δ and α have a significant effect on the distribution of each of the texture statistic distributions. Specific differences arise due to each of the parameters over the five texture statistics and four ice classes tested (Table 2 and 3). The effect of α is more pronounced than that of δ . Adaptive filtering resulted in a significant difference between filtered and unfiltered texture statistics for each ice type tested. In all cases the reduction in variance caused by the adaptive filter was captured by each texture statistic.

Analysis of the multivariate data resulted in four specific conclusions, each directly related to the four research questions:

- Do the conditional parameters δ and α affect discrimination? Significantly better results were obtained at $\delta=1$ than either $\delta=5$ or 9. Significantly better results were obtained at $\alpha=0^\circ$ than either $\alpha=45^\circ$ or 90° .
- Is there a difference between training and cross validation results? Training results were consistently higher than those obtained through cross validation. Generally, the fewer number of variables used in the LDA the greater the agreement between training and cross validation results. We believe that agreement between the two samples indicates the true Kappa Coefficient classification accuracies.

- What is the best set of texture statistics to discriminate SAR ice types? These analyses indicate that the best discrimination ($K\text{-hat}=72.2\%$; $K_s=0.79\%$) is achieved for a set of three texture statistics considered simultaneously. The equivalent Kappa Coefficient of the published results of Holmes *et al.* (1984) ($K\text{-hat}=54.4\%$; $K_s=0.29\%$) were computed for a single (inertia) GLCM statistic. Because the computationally intensive part of the GLCM approach is determining the matrix density functions, the improved accuracies obtained from the multivariate texture discrimination may be warranted.
- What is the effect of adaptive filtering on discrimination accuracy? There was no significant difference in the classification results between filtered and unfiltered images. Examination of the probabilities associated with each sample suggests that the separability of ice classes is actually reduced by filtering, for these data.

The sample size used in these analyses (15 replicates) was selected because of the trade-off inherent in the sampling designs of the GLCMs and the number of replicates from which to conduct hypothesis testing. Each GLCM must be computed from a sample which is representative of the texture field we wish to measure. Because the ice classes consist of similar textures, a larger GLCM sample size (625 pixels) was considered more appropriate than more replicates with fewer pixels in each. The sampling problems inherent in this dichotomy are by no means fully understood and should form part of future research into the application of texture statistics for feature discrimination.

RECOMMENDATIONS

Statistical texture analysis has been studied in a variety of application areas by many different researchers. One of the major drawbacks of this and other research is that results are limited to the data set from which they were derived. Future analysis should consider the statistical significance of developing textural and tonal discriminant functions in one image then applying these functions to scenes of the same features imaged within a particular season. This type of analysis is required to assess the universality and precision of the results obtained here. Comparisons between this work and those published by other researchers using a single image must be constrained to the identification of common trends, not a quantitative assessment of the merits of different approaches. Differences can be attributable to sample size (i.e., Holmes *et al.* (1984) versus these results); statistical testing differences (i.e., Kappa versus summation of the diagonal elements in a confusion matrix); and other variations in the methods used.

To meet the requirements of the operational sea ice community, it is important that a solution be found which will allow semi-automatic classification of orbital SAR imagery. In meeting the requirements of this challenge, we offer a few simple considerations:

- A thorough comparison of several textural and tonal classification algorithms for sea ice is required. We recommend an evaluation of the relative utility of different algorithms compared over the same scene, and a measure of the robustness of each method, by applying each to other images of the same scene. Analysis of tonal versus textural robustness to changes in range dependent variations must be extended beyond the preliminary analysis conducted by Barber *et al.* (1990).
- Classification algorithms must be seasonally adjusted. This means field validation studies must be mounted which relate classification algorithm performance with seasonal descriptions of sea ice. Livingstone *et al.* (1987) offer an excellent nomenclature and time line (winter, early melt, melt onset, advanced melt, and freeze-up) based on the recent thermal history of the ice. We suggest this nomenclature be adopted and that a concerted effort be made to evaluate the within to between season variations in SAR signatures of sea ice, either through *in situ* scatterometer measurements or empirical studies. Synergistic data, particularly thermal and passive microwave, should be evaluated as a means of identifying the onset and change of this seasonality.

- With improvements in relative SAR calibration, tonal classifiers should be thoroughly evaluated, specifically in the context of a multivariate classification with textural measures and association with seasonally dependent look-up tables (previous point).
- To satisfy the operational requirements of the sea ice community, it is important to develop classifiers which capture the essential textural information but are computationally fast. We also must not overlook the real potential for improvements in computer speed within the next two to five years when researching the utility of texture in sea ice classification.

Multi-disciplinary field verification studies on SAR scattering from sea ice should continue to provide excellent quantitative information on the backscattering properties of sea ice. Within these studies an emphasis should be placed on linking the results of micro-scale modeling with macro-scale digital image classification as a function of season. Of paramount importance is development of an understanding of the specific backscattering variables, and their spatial arrangements, which give rise to the texture inherent in SAR imagery of sea ice.

ACKNOWLEDGMENTS

We would like to acknowledge the Atmospheric Environment Service, Ice Branch, Ottawa, Canada for the surface validation data. The Ice Applications Section of the Canada Centre for Remote Sensing, Ottawa, Canada provided the data used throughout these analyses. Our colleagues, Mr. D. Dunlop and Mr. P. Gong, provided timely assistance with components of the computer software and the coding of the Kappa Coefficient. Ms. S. Digby-Argus provided a constructed review of the manuscript. This research was supported by a Centre of Excellence grant from the Province of Ontario to the Institute for Space and Terrestrial Science, and an NSERC Operating Grant to E. LeDrew.

REFERENCES

- Barber, D. G., 1989. *Texture Measures for SAR Sea Ice Discrimination: An Evaluation of Univariate Statistical Distributions*. Earth Observations Lab Technical Report Series ISTS-EOL-TR89-005. Department of Geography, University of Waterloo, Ont. 56 p.
- Barber, D. G. and E. F. LeDrew, 1989. Multivariate Analysis of Texture Statistics for SAR Sea Ice Discrimination. *Proceeding of the International Geoscience and Remote Sensing Society*. Vancouver, B.C. 2, 759-762.
- Barber, D. G., D. D. Johnson, and E. F. LeDrew, 1990. Measuring Climatic State Variables from SAR Images of Sea Ice: The SIMS SAR Validation Site in Lancaster Sound. Presented at the First Circumpolar Conference on Remote Sensing, Yellowknife, NWT. Currently under review for publication in *Arctic*.
- Bishop, Y. M. M., S. E. Fienberg, and P. W. Holland, 1975. *Discrete Multivariate Analysis: Theory and Practice*. MIT Press, Cambridge, Mass. 557 p.
- Blom, R. G., L. R. Schenck, and R. E. Alley, 1987. What are the Best Radar Wavelengths, Incidence Angles, and Polarizations for Discrimination Among Lava Flows and Sedimentary Rock? A Statistical Approach. *IEEE Trans Geosc. Rem. Sens.*, GE-25 (2), 208-213.
- Burns, B. A., and D. R. Lyzenga, 1984. Textural Analysis as a SAR Classification Tool. *Electromagnetics*, 4, 309-322.
- Burns, B. A., E. S. Kasischke, and D. R. Nuesch, 1982. Extraction of Texture information from SAR Data: Application to Ice and Geological Mapping. *Int. Symp. on Rem. Sens. of Envir. Second Thematic Conference*, Fort Worth Texas. pp. 861-868.
- Connors, R. W., M. M. Trivedi, and C. A. Harlow, 1984. Segmentation of a High-Resolution Urban Scene Using Texture Operators. *Computer Vision, Graphics and Image Processing*, 25, 273-310.
- Connors, R. W., and C. A. Harlow, 1980a. A Theoretical Comparison of Texture Algorithms. *IEEE Transactions on Pattern Analysis and Machine Intelligence*, PAMI-2 (3), 204-222.
- , 1980b. Toward a Structural Textural Analyzer Based on Statistical Methods. *Computer Graphics and Image Processing*, 12, 224-256.

- D'Astous, F., and M. E. Jernigan, 1984. Texture Discrimination based on Detailed Measures of the Power Spectrum. *Seventh International Conference on Pattern Recognition*, pp. 83-86.
- Drinkwater, M. R., and G. B. Crocker, 1988. Modelling Changes in the Dielectric and Scattering Properties of Young Snow-Covered Sea Ice at GHz Frequencies. *Journal of Glaciology*, 34(118), 274-282.
- Durand, M. J., B. J. Gimonet, and J. R. Perbos, 1987. SAR Data Filtering for Classification. *IEEE Trans Geosc. Rem. Sens.*, GE-25 (5), 629-637.
- Franklin, S. E., D. R. Peddle, and J. E. Moulton, 1989. Spectral/Geomorphic Discrimination and Mapping of Terrain: A Study in Gros Morne National Park. *Can. J. of Rem. Sens.*, 15 (1), 28-42.
- Galloway, M. M., 1975. Texture Analysis Using Gray Level Run Lengths. *Computer Graphics and Image Processing*, 4, 172-179.
- Haralick, R. M., K. Shanmugan, and I. Dinstein, 1973. Textural Features for Image Classification. *IEEE Transaction on Systems, Man and Cybernetics*, 6, 610-621.
- Hassner, M., and J. Sklansky, 1980. The Use of Markov Random Fields as Models of Texture. *Computer Graphics and Image Processing*, 12, 357-370.
- Hirose, T. K., L. McNutt, and J. S. Paterson, 1989. A study of textural and Tonal Information for Classifying Sea Ice from SAR Imagery. *Proceeding of the International Geoscience and Remote Sensing Society*. Vancouver, B.C. 2, 747-750.
- Hcolbaek-Hansen, E., H. Thjelmeland, O. M. Johannessen, T. Olausen, and R. Karpuz, 1988. Speckle Reduction and Maximum Likelihood Classification of SAR Images from Sea Ice Recorded during MIZEX 87. *Proceeding of the International Geoscience and Remote Sensing Society*. Vancouver, B.C. 2, 755-758.
- Holmes, Q. A., D. R. Nuesch, and R. A. Shuchman, 1984. Textural Analysis and Real-Time Classification of Sea-Ice Types Using Digital SAR Data. *IEEE Trans. Geos. and Rem. Sens.* GE-22(2) 113-120.
- Holt, B., R. Kwok, and E. Rignot, 1989. Ice Classification Algorithm Development and Verification for the Alaska SAR Facility Using Aircraft Imagery. *Proceeding of the International Geoscience and Remote Sensing Society*. Vancouver, B.C. 2, 751-754.
- Irons, J. R., and G. W. Petersen, 1981. Texture Transforms of Remote Sensing Data. *Remote Sensing of Environment* 11:359-370.
- Kershaw, C. D., 1987. Discrimination Problems for Satellite Images. *Int. J. Remote Sensing*, 8(9), 1377-1383.
- Kim, J. S., R. K. Moore, R. G. Onstott, and S. Gogineni, 1985. Towards Identification of Optimum Radar Parameters for Sea Ice Monitoring. *Journal of Glaciology*, 31(109) 214-219.
- Livingstone, C. E., R. G. Onstott, L. D. Arsenaault, A. L. Grey, and K. P. Singh, 1987. Microwave Sea-Ice Signatures Near the Onset of Melt. *IEEE Trans. on Geosc. Rem. Sens.* GE-25(2). 174-187.
- Ludwig, J. A., and J. F. Reynolds, 1988. *Statistical Ecology*. John Wiley and Sons, New York, 337 p.
- Luther, C. A., J. D. Lyden, R. A. Shuchman, R. W. Larson, Q. A. Holmes, D. R. Nuesch, R. T. Lowry, and C. E. Livingstone, 1982. Synthetic Aperture Radar Studies of Sea Ice. *International Geoscience and Remote Sensing Symposium*. Munich, Germany. 2. 1.1-1.9.
- Lyden, J. D., B. A. Burns, and A. L. Maffett, 1984. Characterization of Sea Ice Types Using Synthetic Aperture Radar. *IEEE Trans. Geos. and Rem. Sens.* GE-22(5) 431-439.
- Manly, B. F. J., 1986. *Multivariate Statistical Methods*. Chapman and Hall, London, 159 p.
- Mather, P., 1987. *Computer Processing of Remotely Sensed Images: An Introduction*. New York, Wiley and Sons, 346 p.
- Matsuyama, T., S. I. Miura, and M. Nagao, 1983. Structural Analysis of Natural Textures by Fourier Transformation. *Computer Graphics and Image Processing*, 24, 347-362.
- McNutt L., and T. Viehoff (eds.), 1989. *Program for International Polar Oceans Research (PIPOR)*. ERS-1 Research Plan. unpublished.
- Nichols, A. D., J. W. Wilhelm, T. W. Gaffield, R. D. Inkster, and S. K. Leung, 1986. A SAR for Real-Time Ice Reconnaissance. *IEEE Trans Geosc. Rem. Sens.*, GE-24(3), 383-389.
- Pultz, T. J., and R. J. Brown, 1987. SAR Image Classification of Agricultural Targets Using First-And Second-Order Statistics. *Can. J. of Rem. Sens.*, 13(12), 85-91.
- Raney, R. K., 1989. Toward Quantitative Observations from Synthetic Aperture Radar. *Proceeding of the International Geoscience and Remote Sensing Society*. Vancouver, B.C. 1, 12-15.
- Roan, S. J., and J. K. Aggarwal, 1987. Multiple Resolution Imagery and Texture Analysis. *Pattern Recognition*, 20(1), 17-31.
- Schwaller, M. R., 1987. A Geobotanical Investigation Based on Linear Discriminant and Profile Analyses of Airborne Thematic Mapper Simulator Data. *Remote Sensing of Environment*, 23, 23-34.
- Shanmugan, K. S., V. Narayanan, V. S. Frost, J. A. Stiles, and J. C. Holtzman, 1981. Textural Features for Radar Image Analysis. *IEEE Trans Geosc. Rem. Sens.*, GE. 19(3), 153-156.
- Shokr, M. E., 1989. Texture Measures for Sea-Ice Classification from Radar Images. *Proceeding of the International Geoscience and Remote Sensing Society*. Vancouver, B.C. 2, 763-768.
- Shuchman, R. A., B. A. Burns, C. C. Wackerman, R. G. Onstott, and J. D. Lyden, 1987. Progress on Digital Algorithms for Deriving Sea Ice Parameters from SAR data. *Proceeding of the International Geoscience and Remote Sensing Society*. Ann Arbor, Mich. 2, 1131-1133.
- Shuchman, R. A., C. C. Wackerman, A. L. Maffett, R. G. Onstott, and L. L. Sutherland, 1989. The discrimination of Sea Ice Types Using SAR Backscatter Statistics. *Proceeding of the International Geoscience and Remote Sensing Society*. Vancouver, B.C. 381-385.
- Steiner D., K. Baumberger, and J. Maurer, 1971. Computer-Processing and Classification of Multi-Variate Information from Remote Sensing Imagery. A Review of the Methodology as Applied to a Sample of Agricultural Crops. *Sixth International Symposium on Remote Sensing of the Environment*. Ann Arbor Mich. 895-907.
- Sun, C., and W. G. Wee, 1982. Neighbouring Gray Level Dependence Matrix for Texture Classification. *Computer Vision, Graphics and Image Processing*, 23, 341-352.
- Ulaby, F. T., R. K. Moore, and A. K. Fung, 1986. *Microwave Remote Sensing: Active and Passive*. Vol III. Addison-Wesley Publishing Company. Massachusetts. 2162 p.
- Ulaby, F. T., F. Kouyate, B. Brisco, and T.H. Lee Williams, 1986. Textural Information in SAR Images. *IEEE Trans Geosc. Rem. Sens.*, GE. 24(2), 235-245.
- Wechsler, H., and M. Kidode, 1979. A Random Walk Procedure for Texture Discrimination. *IEEE Transactions on Pattern Analysis and Machine Intelligence*, PAMI-1(3), 272-280.
- Weszka, J. S., C. R. Dyer, and A. Rosenfeld, 1976. A Comparative Study of Texture Measures for Terrain Classification. *IEEE Transactions on Systems, Man, and Cybernetics*, SMC-6(4), 269-285.
- Wilkinson, L., 1987. *SYSTAT: The System for Statistics*. SYSTAT, Inc., Evanston, Illinois.
- Williams, B. K., and K. Titus, 1983. Some Observations on the Use of Discriminant Analysis in Ecology. *Ecology*, 64(5), 1283-1291.

(Received 20 October 1989; revised and accepted 19 June 1990)

XVII ISPRS CONGRESS

August 2-14, 1992

Washington, DC



Mark your calendars now and plan to attend the XVII Congress of the International Society for Photogrammetry and Remote Sensing. For information, call: 703-648-5110 or write P.O. Box 7147, Reston, VA 22091-7147.